

Photon-ALP oscillations from a blazar to us up to 1000 TeV

Giorgio Galanti*

INAF, Osservatorio Astronomico di Brera, Via Emilio Bianchi 46, I – 23807 Merate, Italy

Fabrizio Tavecchio†

INAF, Osservatorio Astronomico di Brera, Via Emilio Bianchi 46, I – 23807 Merate, Italy

Marco Roncadelli‡

INFN, Sezione di Pavia, Via A. Bassi 6, I – 27100 Pavia, Italy, and INAF

Carmelo Evoli§

*Gran Sasso Science Institute, Viale Francesco Crispi 7, I – 67100 L'Aquila, Italy,
and INFN, Laboratori Nazionali del Gran Sasso (LNGS), 67100 Assergi, L'Aquila, Italy*

Prompted by the increasing interest of axion-like particles (ALPs) for very-high-energy (VHE, 100 GeV $\lesssim \mathcal{E} \lesssim 100$ TeV) astrophysics, we have considered a full scenario for the propagation of a VHE photon/ALP beam emitted by a BL Lac and reaching us in the light of the most up-to-date astrophysical information and for energies up to 1000 TeV. During its trip, the beam – generated in a small region of a BL Lac jet – crosses a variety of magnetic structures in very different astronomical environments: the BL Lac jet, the host elliptical galaxy, the extragalactic space and the Milky Way. We have taken an effort to model all these magnetic fields in the most realistic fashion, even if the morphology and strength of the extragalactic magnetic field are basically unknown. Still, we believe that the best approximation remains the one based on a domain-like network based on the picture of primeval galactic outflows, further amplified by turbulence. Basically, \mathbf{B} has nearly the same strength in all domains – which means around each galaxy – but its direction changes randomly from one domain to the next, as a consequence of the fact that neighboring galaxies are uncorrelated. While at presently accessible energies the jump of \mathbf{B} across the domain edges gives rise to no problem, in order to cope with the needs of the next generation of VHE observatories we had to use a more elaborate version. We have first evaluated the photon survival probability along the beam from the BL Lac to us. Next – assuming an intrinsic spectrum with a power law exponentially truncated at a fixed cut-off energy – we have evaluated the observed spectrum of Markarian 501, the extreme BL Lac 1ES 0229+200 and a similar source located at $z = 0.6$ up to 1000 TeV. In the first two cases, for the highest energy points we find a better agreement with respect to conventional physics. In the latter case – after a minimum at $\mathcal{E} \simeq 3$ TeV – we find a surprising very high peak at $\mathcal{E} = (10 - 30)$ TeV depending on the line of sight. We show that this is ultimately a consequence of the photon to ALP conversion inside the BL Lac: because at high energy photon dispersion on the CMB dominates in the extragalactic space, this prevents most of those ALPs to convert to photons until they enter the Galaxy, where its strong magnetic field allows them to become photons. Finally, our scenario leads to two predictions that can be tested in the near future by γ -ray observatories like CTA, HAWC, GAMMA- 400, LHAASO, TAIGA-HiSCORE and HERD. One is the energy oscillations in the observed spectrum (provided that the detector has enough energy resolution), to be traced back to the photon dispersion on the CMB. The other is the possible detection of the unexpected peak in BL Lac spectra at $\mathcal{E} = (10 - 30)$ TeV. In addition, for our benchmark values of the ALP mass and its two-photon coupling, our ALP can be detected in dedicated laboratory experiments like the upgrade of ALPS II at DESY, the planned IAXO and STAX experiments, as well as with other techniques developed by Avignone and collaborators.

Introduction – Everybody knows that the atmosphere is fully opaque to gamma rays. While this is good for us – otherwise life would be impossible on Earth – for many years it has been regarded as a stumbling block for gamma-ray

*Electronic address: gam.galanti@gmail.com

†Electronic address: fabrizio.tavecchio@brera.inaf.it

‡Electronic address: marco.roncadelli@pv.infn.it

§Electronic address: carmelo.evoli@gssi.it

observations from the ground. Only about twenty years ago or so has it been realized that the atmospheric opacity can be an opportunity for ground-based gamma-ray observations in the very-high-energy band (VHE, $100 \text{ GeV} \lesssim \mathcal{E} \lesssim 100 \text{ TeV}$). Basically, the idea is as follows. When a VHE photon coming from a blazar – AGN with a jet occasionally pointing towards us – strikes the atmosphere, it gives rise to a very energetic shower including charged particles and secondary photons. Because the charged particles have a speed slightly higher than the velocity of light in the atmosphere, they produce a flash of violet Cherenkov light about 8 Km above the Earth. Such a Cherenkov light can be observed with one or more 10 meter class telescopes, and from the shape of the shower and the specific properties of the Cherenkov light one can infer both the energy and the arrival direction of the primary photon by means of the Imaging Atmospheric Cherenkov Telescopes (IACTs). Nowadays, three of them are operative: H.E.S.S. (High Energy Stereoscopic System) [1], MAGIC (Major Atmospheric Gamma Imaging Cherenkov Telescopes) [2] and VERITAS (Very Energetic Radiation Imaging Telescope Array System) [3], which have detected blazars out to redshift $z \simeq 0.9$ and reach energies up to $\mathcal{O}(10 \text{ TeV})$. But the upcoming CTA (Cherenkov Telescope Array) – consisting of about fifty IACTs in the south site and about thirty IACTs in the north site – will be able to probe the whole VHE band with great sensitivity and full sky coverage [4].

Unfortunately, this kind of observations suffer from another sort of opacity: the *extragalactic background light* (EBL). This is the infrared/optical/ultraviolet light emitted by the whole population of galaxies during their cosmic evolution (for a review, see [5]). As a consequence, a VHE photon of energy \mathcal{E} can scatter off an EBL photon of energy ϵ , thereby producing an e^+e^- pair according to the Breit-Wheeler process $\gamma + \gamma \rightarrow e^+ + e^-$ [6, 7]. It can be shown that its cross-section gets maximized for [8]

$$\epsilon \simeq \left(\frac{900 \text{ GeV}}{\mathcal{E}} \right) \text{eV} . \quad (1)$$

Therefore, we see that for $100 \text{ GeV} \lesssim \mathcal{E} \lesssim 100 \text{ TeV}$ we get $0.009 \text{ eV} \lesssim \epsilon \lesssim 9 \text{ eV}$: just the energy range of the sky dominated by the EBL. So, what happens is that the optical depth increases both with z and \mathcal{E} [9], thereby progressively more and more limiting the observations at VHE as either z or \mathcal{E} (or both) get larger and larger (for an updated quantitative account, see [10]).

A partial way out of this difficulty was first proposed in 2007 in term of photon-ALP oscillations in the extragalactic space [11]. ALPs are axion-like particles – whose properties will be summarized below – but the main point is that they totally avoid EBL absorption. In 2008, a complementary possibility has been put forward: photon-to-ALP conversion inside a blazar and ALP-to-photon reconversion in the Galaxy [12].

The aim of this Letter is to contemplate all the magnetic environments at once crossed by the photon/ALP beam – blazar jet, host galaxy, extragalactic space and the Milky Way – so as to provide the most accurate description as possible according to the present state of the art. A first attempt along the same direction has been done in 2009 [13], using however some simplistic assumptions in the lack of a better knowledge: in this field the progress since 2009 has really been impressive.

As a matter of fact, we identify five points that can and should be improved.

- The magnetic field in the blazar jet should be described by an analytic model rather than by a domain-like model as in [13].
- Rather than assuming some value for the photon-ALP conversion probability as in [13], we compute it in terms of realistic values of the relevant parameters.
- New bounds on the model parameters has been derived.
- The photon dispersion in the CMB – whose relevance has been realized in 2015 [14] – plays a crucial role in the description of the extragalactic photon/ALP propagation in order to deal with energies up to 1000 TeV, as required by the next generation of gamma ray detectors (more about this, towards the end of the Letter).
- The EBL model has been improved in 2017 [15].
- The Galactic magnetic field has been modeled in considerable detail by Jansson and Farrar in 2012 [16, 17].

Thus, we will evaluate the total VHE photon survival probability within the full scenario, namely from their origin in the BL Lacs jet, during their propagation inside the jet, within the host galaxy and the extragalactic space, and finally inside the Milky Way to us by taking the above points into account. In addition, assuming a realistic emitted spectrum for three BL Lacs – Markarian 501, 1ES 0229+200 and a similar source located at $z = 0.6$ – we derive the observed spectrum up to 1000 TeV.

General features of axion-like particles (ALPs) – As we said, a key role is played in our considerations by axion-like particles (ALPs). They are spin-zero, neutral and extremely light pseudo-scalar bosons, to be denoted by a throughout this Letter. They are attracting growing interest, especially because they are a natural prediction of superstring theories (for a review, see [18, 19]). ALPs closely resemble the axion (for a review, see [20]) apart from two facts: 1) possible couplings to fermions and gluons are discarded for our purposes, and only their two-photon coupling $g_{a\gamma\gamma}$ is taken into account; 2) the ALP mass m_a is totally unrelated to $g_{a\gamma\gamma}$. As a result, ALPs are described by the Lagrangian

$$\mathcal{L}_{\text{ALP}} = \frac{1}{2} \partial^\mu a \partial_\mu a - \frac{1}{2} m_a^2 a^2 + g_{a\gamma\gamma} a \mathbf{E} \cdot \mathbf{B} , \quad (2)$$

where \mathbf{E} and \mathbf{B} denote the electric and magnetic components of the electromagnetic tensor $F^{\mu\nu}$. As far as our considerations are concerned, in the presence of an *external* magnetic field \mathbf{B} field the mass matrix of the $\gamma - a$ system is off-diagonal (the electric field \mathbf{E} in (2) pertains to a propagating photon). As a consequence, the propagation eigenstates differ from the interaction eigenstates: hence $\gamma \leftrightarrow a$ oscillations take place, since ALPs have no chance to decay since for values of m_a to be considered below the time for the process $a \rightarrow \gamma + \gamma$ is much longer than the age of the Universe [21–23]. Because the $\gamma\gamma a$ interaction Lagrangian is $g_{a\gamma\gamma} a \mathbf{E} \cdot \mathbf{B}$ and \mathbf{E} is orthogonal to the photon momentum \mathbf{k} only the component \mathbf{B}_T of \mathbf{B} , transverse to \mathbf{k} , couples to ALPs.

We shall henceforth consider throughout this Letter a photon/ALP beam of energy \mathcal{E} which propagates from a BL Lac towards us along the y direction, in the presence of an external magnetic field \mathbf{B} which depends on the considered environment.

When \mathbf{B} is strong – like in the case of the jet of BL Lacs – also the one-loop QED vacuum polarization must be taken into account, which is described by the effective Lagrangian [23–26]

$$\mathcal{L}_{\text{HEW}} = \frac{2\alpha^2}{45m_e^4} \left[(\mathbf{E}^2 - \mathbf{B}^2)^2 + 7(\mathbf{E} \cdot \mathbf{B})^2 \right] , \quad (3)$$

where α is the fine-structure constant and m_e is the electron mass. Note that \mathcal{L}_{HEW} holds true for $\mathcal{E} \gg m_e$ [14]. In addition, for weak magnetic fields – namely the ones filling the extragalactic space $\mathcal{O}(1 \text{ nG})$ (more about this later) – and for $\mathcal{E} \gtrsim \mathcal{O}(10 \text{ TeV})$ the photon dispersion on the cosmic microwave background (CMB) plays a leading role [14], and we will include it. Throughout this Letter we use the rationalized system with natural units.

From Eqs. (2) and (3) it is possible to derive a propagation equation for the photon/ALP beam. Actually, since (as we shall see) we will be dealing with the situation $m_a \ll \mathcal{E}$, such an equation reduces to a Schrödinger-like equation with time replaced by y [23]: see e.g. [27, 28] to which we refer the reader for more details. Thus, the photon/ALP beam is formally described as a three-level ($A_x(y)$, $A_z(y)$ and $a(y)$) nonrelativistic quantum system, where $A_x(y)$ and $A_z(y)$ denote the photon amplitudes with polarization along the x and z axis, respectively, while $a(y)$ is the amplitude associated with the ALP. Accordingly, the most important quantity which quantifies the beam propagation is the *transfer matrix* of the Schrödinger-like equation, which will be referred to as \mathcal{U} : it is the solution $\mathcal{U}(\mathcal{E}; y, y_0)$ such that $\mathcal{U}(\mathcal{E}; y_0, y_0) = 1$.

A concept that is instrumental for our subsequent analysis is that of *strong mixing*. To this end, we define the *low-energy threshold* \mathcal{E}_L and the *high-energy threshold* \mathcal{E}_H as

$$\mathcal{E}_L \equiv \frac{|m_a^2 - \omega_{\text{pl}}^2|}{2g_{a\gamma\gamma} B_T} , \quad (4)$$

and

$$\mathcal{E}_H \equiv g_{a\gamma\gamma} B_T \left[1.42 \cdot 10^{-4} \left(\frac{B_T}{B_{\text{cr}}} \right)^2 + 0.522 \cdot 10^{-42} \right]^{-1} , \quad (5)$$

respectively. In Eq. (4) ω_{pl} is the plasma frequency – related to the electron density n_e by $\omega_{\text{pl}} = 3.69 \cdot 10^{-11} (n_e/\text{cm}^{-3})$ – whereas in Eq. (5) $B_{\text{cr}} \simeq 4.41 \cdot 10^{13} \text{ G}$ is the critical magnetic field, and the last terms accounts for photon dispersion on the CMB [14]. Now, the strong mixing regime takes place for $\mathcal{E}_L \lesssim \mathcal{E} \lesssim \mathcal{E}_H$: It can be shown that within that regime the $\gamma \rightarrow a$ and $a \rightarrow \gamma$ conversion probability is independent both of \mathcal{E} and m_a , and in addition becomes maximal. Further, what happens is that outside the strong mixing regime the $\gamma \rightarrow a$ and $a \rightarrow \gamma$ conversion probability rapidly decreases in an oscillatory fashion with a decreasing oscillation length as either \mathcal{E} gets smaller and smaller than \mathcal{E}_L or \mathcal{E} gets larger and larger than \mathcal{E}_H . As a consequence, the oscillatory behaviour can be observed with the present capabilities only close to \mathcal{E}_L or \mathcal{E}_H (for a detailed discussion, see [28]).

A final warning is in order. Obviously, ALPs have spin 0 while photons have spin 1, and so the presence of an external magnetic field \mathbf{B} is absolutely compelling in order for oscillations to take place. For this reason, particular attention will be paid to the magnetic field present in any environment crossed by our photon/ALP beam.

Parameter space – Before plunging into our analysis, it is obviously compelling to know the allowed ranges of the two photon coupling $g_{a\gamma\gamma}$ and the ALP mass m_a .

The negative result of the CAST (CERN Axion Solar Telescope) experiment sets the most up-to-date upper bound on the ALP-photon coupling $g_{a\gamma\gamma} < 0.66 \cdot 10^{-10} \text{ GeV}^{-1}$ for $m_a < 0.02 \text{ eV}$ at the 2σ level [29]. Exactly the same bound at the same confidence level has been obtained from the study of globular cluster stars [30].

Let us next focus our attention on the bounds on $g_{a\gamma\gamma}$ which depend on m_a . Basically, the involved strategy is to rely upon the absence of the characteristic energy oscillating behavior around \mathcal{E}_L . Accordingly, several bounds have been derived [31–38] in this way. The most relevant ones come from the analysis of the radio galaxy NGC 1275 in the central region of the Perseus cluster. In 2016 by the Fermi/LAT collaboration excluded the region $g_{a\gamma\gamma} \lesssim 5 \cdot 10^{-12} \text{ GeV}^{-1}$ at the 2σ level for $5 \cdot 10^{-10} \text{ eV} \lesssim m_a \lesssim 5 \cdot 10^{-8} \text{ eV}$ [35]. Subsequently, in 2018 Malyshev *et al.* excluded the region $g_{a\gamma\gamma} \lesssim 8 \cdot 10^{-13} \text{ GeV}^{-1}$ at the 2σ level for $10^{-10} \text{ eV} \lesssim m_a \lesssim 10^{-8} \text{ eV}$ [38]. So, they can be avoided altogether by taking $m_a \lesssim 10^{-10} \text{ eV}$.

A quite different story concerns the bound derived from the lack of detection of ALPs supposedly emitted by the supernova SN1987A. They were assumed to convert into gamma-rays of the same energy in the Galactic magnetic field, and so they ought to have been observed by the Gamma-Ray Spectrometer (GRS) aboard the Solar Maximum Mission (SMM) satellite, even though its line of sight was orthogonal to the direction to supernova SN1987A.

In 1996 two papers almost simultaneously appeared which analyzed the GRS data and from the lack of gamma-ray detection coming from SN1987A a bound on $g_{a\gamma\gamma}$ for nearly massless ALPs was derived [39, 40]. Both of them address the Primakoff ALP production process inside the protoneutron star (PNS) just before the bounce, but are actually framed in the vacuum plus the condition that electrons are fully degenerate, which are correctly supposed to play no dynamical role because of Pauli blocking. Obviously, this is clearly an oversimplification. In 2015 a much more detailed follow-up analysis of the same issue appeared. Again, it considers the Primakoff ALP production process inside the protoneutron star (PNS) just before the bounce exactly in the same fashion of the previous papers, and takes into account strong interactions *only* to the extent that they produce a small reduction of the nucleon mass and a slight proton degeneracy [41]. Unfortunately, also this paper neglects important effects.

Some criticism of the above papers has already been pointed out already in 2009 [13] – which also applies to [41] – which we refrain from repeating here. Nevertheless [41] lends itself to further criticism. 1) The Primakoff ALP production mechanism is computed by means of the usual propagator employing the Minkowski metric, in spite of the fact that it must be treated with a metric which takes into account the properties of the medium, namely nuclear matter at twice the nuclear saturation density and temperature $T \simeq 40 \text{ K}???$, – $> 20\text{--}30 \text{ MeV}$, which is obviously very different from the Minkowski one of ordinary vacuum (this point is explained in great detail in Raffelt’s book [42]). Alternatively, one may follow the approach outlined in [43], but extending it to finite temperatures. 2) Moreover, the PNS typically has a rotation period of the order of a millisecond, hence it is a highly non-inertial reference frame, so that the Minkowski metric should be changed. 3) The effects of magnetic fields as strong as $B = (10^{12} - 10^{16}) \text{ G}$ – apart from those already mentioned in [13] – are simply discarded. Presumably, it gives rise to the same effect considered in [23] in a somewhat different situation – $\gamma \rightarrow a$ conversions in the magnetosphere of a pulsar – namely a strong suppression of the $\gamma \rightarrow a$ conversions. For all these reasons, we do not trust the the claimed bound $g_{a\gamma\gamma} \lesssim 5.3 \cdot 10^{-12} \text{ GeV}^{-1}$ for $m_a \lesssim 4.4 \cdot 10^{-10} \text{ eV}$ [41].

Thus, in order to be specific we choose as benchmark values $g_{a\gamma\gamma} = 10^{-11} \text{ GeV}^{-11}$ and $m_a \simeq 10^{-10} \text{ eV}$.

Photon/ALP propagation in the jet – We denote by \mathcal{R}_{VHE} the region where the VHE photons originate inside the BL Lac jet, letting y_{VHE} be its distance from the central black hole (BH). So, our first step is to evaluate the transfer matrix over the jet region \mathcal{R}_{jet} between y_{VHE} and the end of the jet y_{jet} , which we denote as $\mathcal{U}_{\mathcal{R}_{\text{jet}}}(\mathcal{E}; y_{\text{jet}}, y_{\text{VHE}})$.

Here we closely follow our results concerning the same problem as derived in a previous Letter [44]. We start by recalling that the region \mathcal{R}_{VHE} is rather far from the central BH, and the jet axis is supposed to coincide with the direction y . In order to evaluate the photon/ALP beam propagation inside the jet we must know three quantities: 1) the distance y_{VHE} , 2) the transverse magnetic field profile $B_{T,\mathcal{R}_{\text{jet}}}(y)$ from y_{VHE} to y_{jet} , 3) the electron density profile $n_{e,\mathcal{R}_{\text{jet}}}(y)$ from y_{VHE} to y_{jet} . Realistic values for these quantities can be derived from Synchrotron Self Compton (SSC) diagnostics as applied to the *spectral energy distribution* (SED) of BL Lacs [45]. Inside \mathcal{R}_{VHE} we get $B_{T,\mathcal{R}_{\text{VHE}}} = (0.1 - 1) \text{ G}$ and in order to be definite we choose $B_{T,\mathcal{R}_{\text{VHE}}} = 0.5 \text{ G}$. Moreover, we find $n_{e,\mathcal{R}_{\text{VHE}}} \simeq 5 \cdot 10^4 \text{ cm}^{-3}$, leading in turn to a plasma frequency of $\omega_{\text{pl}} \simeq 8.25 \cdot 10^{-9} \text{ eV}$. Although there is no direct way to infer a precise value of y_{VHE} , we can estimate it from the size of \mathcal{R}_{VHE} – which is assumed to be a measure of the jet cross-section – thus finding $y_{\text{VHE}} = (10^{16} - 10^{17}) \text{ cm}$. For definiteness, we shall take $y_{\text{VHE}} \simeq 3 \cdot 10^{16} \text{ cm}$. Once produced, VHE photons propagate unimpeded out to $y_{\text{jet}} \simeq 1 \text{ kpc}$ where they leave the jet, entering the host galaxy. More specifically, within \mathcal{R}_{jet} what

is relevant is the toroidal part of the magnetic field which is transverse to the jet axis [46–48]. Its profile reads

$$B_{T,\mathcal{R}_{\text{jet}}}(y) = \frac{B_{T,\mathcal{R}_{\text{VHE}}} y_{\text{VHE}}}{y}. \quad (6)$$

As far as the electron density profile is concerned, due to the conical shape of the jet our expectation is

$$n_{e,\mathcal{R}_{\text{jet}}}(y) = n_{e,\mathcal{R}_{\text{VHE}}} \left(\frac{y_{\text{VHE}}}{y} \right)^2. \quad (7)$$

By knowing the above quantities, it is possible to calculate the entire propagation process of the photon/ALP beam within the jet, namely $\mathcal{U}_{\mathcal{R}_{\text{jet}}}(\mathcal{E}; y_{\text{jet}}, y_{\text{VHE}})$.

Some remarks are in order. In the first place, we have provided a detailed modeling of the magnetic field in a BL Lac jet, which greatly differs from the domain-like one employed in the original full scenario for PKS 2155-304 [13]. Moreover, we stress that in \mathcal{R}_{jet} we consider the photon/ALP beam in a frame co-moving with the jet, so that we must apply the transformation $\mathcal{E} \rightarrow \gamma\mathcal{E}$ to the beam in order to go to a fixed frame – as we will do in the next regions – with γ being the Lorentz factor. We take $\gamma = 15$.

Photon/ALP beam propagation in the host galaxy – All the three considered blazars are hosted by an elliptical galaxy, which we denote by $\mathcal{R}_{\text{host}}$. Although very little is known about the magnetic field in this kind of galaxies, it has been argued that supernova explosions and stellar motion give rise to a turbulent \mathbf{B} in $\mathcal{R}_{\text{host}}$ which can be described by a domain-like model with average strength $B \simeq 5 \mu\text{G}$ and coherence length $L_{\text{dom}} \simeq 150 \text{ pc}$ [49]. As we have shown elsewhere [50], its effect on the photon/ALP beam is totally negligible, and so we ignore it. Therefore, denoting by $y_{\text{in,host}} \equiv y_{\text{jet}}$ and by $y_{\text{out,host}}$ the points on the y axis where the beam enters and exits from the host galaxy, respectively, we have $\mathcal{U}_{\mathcal{R}_{\text{host}}}(\mathcal{E}; y_{\text{out,host}}, y_{\text{in,host}}) = 1$.

Photon/ALP beam propagation in the extragalactic space – We let \mathcal{R}_{ext} be the region where the photon/ALP beam propagates in the extragalactic space, i.e. from $y_{\text{out,host}}$ up to the border of the Milky Way y_{MW} . Clearly, the beam behaviour in \mathcal{R}_{ext} is affected by the morphology and strength of the extragalactic magnetic field \mathbf{B}_{ext} . Unfortunately, almost nothing is known about it, and many configurations for \mathbf{B}_{ext} have been proposed [53–56]. Current limits restrict B_{ext} to the range $10^{-7} \text{ nG} \leq B_{\text{ext}} \leq 1.7 \text{ nG}$ on the scale of $\mathcal{O}(1 \text{ Mpc})$ [57–59].

According to the current wisdom, \mathbf{B}_{ext} is modeled as a domain-like network, in which \mathbf{B}_{ext} is assumed to be homogeneous over a whole domain of size L_{dom} equal to its coherence length, with \mathbf{B}_{ext} changing randomly and abruptly its direction from one domain to the next but keeping approximately the same strength [53, 54]. As a matter of fact, this picture relies upon a very plausible physical model, ultimately based on galactic outflows. Specifically, quasar outflows are supposed to be responsible for the formation of the \mathbf{B}_{ext} seeds, which are next amplified by turbulence [60–62]. Alternatively, it has been suggested that outflows from dwarf galaxies produce the seeds of \mathbf{B}_{ext} , which is again amplified by turbulence (note that dwarf galaxies outnumber spiral galaxies by a factor of 10) [63]. In either case, the expectation is $B_{\text{ext}} = \mathcal{O}(1 \text{ nG})$ on the scale $L_{\text{dom}} = \mathcal{O}(1 \text{ Mpc})$. We stress that above domain-like model for \mathbf{B}_{ext} is indeed in line with the considered physical scenario: its cell-like morphology arises from their galactic origin, \mathbf{B}_{ext} has nearly the same strength in all domains – which means around each galaxy – since the latter have nearly the same properties, and the random change of the \mathbf{B}_{ext} direction from one domain to the next simply arises from the fact that neighboring galaxies are uncorrelated. Needless to say, the variation of the \mathbf{B}_{ext} direction is physically smooth across the domain edges, but it is taken constant in each whole domain – thereby giving rise to a jump in the components of \mathbf{B}_{ext} across the domain edges – simply because in this way the beam propagation inside each domain becomes trivial to solve. This model will be referred to for obvious reasons as *domain-like sharp-edges* (DLSHE) model.

What about the above unphysical jump? Let us denote by l_{osc} the $\gamma \leftrightarrow a$ oscillation length and by $P_{\gamma \rightarrow a}(L_{\text{dom}})$ the $\gamma \rightarrow a$ conversion probability within a single domain. Then, as long as $l_{\text{osc}} \gg L_{\text{dom}}$ the considered model yields correct physical results. The reason is that in this case only a small fraction of a single oscillation is *coherently* affected by \mathbf{B} in one domain, and so $P_{\gamma \rightarrow a}(L_{\text{dom}})$ becomes insensitive to the *shape* of the magnetic domains and does not feel the jump in question. This is the typical situation encountered so far. In fact, presently operating IACTs reach energies up to $\mathcal{E} = \mathcal{O}(10 \text{ TeV})$. But we are interested in energies up to $\mathcal{E} = \mathcal{O}(100 \text{ TeV})$, and this fact brings about a big difference. As mentioned previously, for $\mathcal{E} \gtrsim \mathcal{O}(10 \text{ TeV})$ the photon dispersion on the CMB [14] becomes dominant, and we have to include it. What happens is that – because of the latter term – l_{osc} decreases as \mathcal{E} increases, and in particular it is found that $l_{\text{osc}} \lesssim \mathcal{O}(1 \text{ Mpc})$ for $\mathcal{E} \gtrsim \mathcal{O}(40 \text{ TeV})$ [51, 52]. This means that the $\gamma \leftrightarrow a$ oscillations probe the whole magnetic field structure – and not just a small part of it as in the cases considered so far – so that the discontinuities in the \mathbf{B}_{ext} components of the original DLSHE model give rise to unphysical results. A way out of this difficulty is to smooth out the sharp edges, thereby allowing the components of \mathbf{B}_{ext} to be continuous across

the domain edges [28, 51]. Although there are many ways to implement such an idea, a *linear smoothing* seems the simplest possibility, which has been called *domain-like smooth-edges* (DLSME) model and worked out in full detail in [28]. We denote by σ the smoothing parameter which measures the path that the photon/ALP beam spends in the smoothed region of a single domain: e.g. $\sigma = 0.2$ means that the beam propagates in the constant angle region for 80% of its path and in the varying angle region for 20%. In order to be definite, we shall take $\sigma = 0.2$. We also let the length of L_{dom} vary according to a power law distribution function $\propto L_{\text{dom}}^{-1.2}$ inside the range 0.2 Mpc – 10 Mpc, so that $\langle L_{\text{dom}} \rangle = 2$ Mpc – which is in agreement both with the considered physical scenario and with the present bounds [58].

Finally, we stress that – because of the random direction of \mathbf{B}_{ext} in every domain – the photon/ALP beam propagation becomes a stochastic process, and so what we actually observe is only a *single realization* of that process.

Coming back to photon/ALP beam propagation in \mathcal{R}_{ext} , it is discussed within the theoretical framework developed in [28, 52], where the most recent data about the extragalactic background light (EBL) are employed [15]. Accordingly, we denote by $\mathcal{U}_{\mathcal{R}_{\text{ext}}}(\mathcal{E}; y_{\text{MW}}, y_{\text{out,host}})$ the corresponding transfer matrix of the photon/ALP beam.

Owing to $\gamma \leftrightarrow a$ oscillations, photons acquire a split personality: when they behave like true photons they suffer EBL absorption, but when they behave as ALPs absorption is totally absent. As a result, the effective optical depth $\tau_{\text{ALP}}(\mathcal{E}, z)$ is larger than in conventional physics. The crux of the argument is that the photon survival probability is now

$$P_{\gamma \rightarrow \gamma}^{\text{ALP}}(\mathcal{E}, z) = \exp[-\tau_{\text{ALP}}(\mathcal{E}, z)] , \quad (8)$$

and even a small increase of $\tau_{\text{ALP}}(\mathcal{E}, z)$ produces a large increase of $P_{\gamma \rightarrow \gamma}^{\text{ALP}}(\mathcal{E}, z)$ as compared to conventional physics.

Before closing this Section, we would like to add some remarks about our choice of the extragalactic magnetic field.

A new approach to $\gamma \rightarrow a$ oscillations in extragalactic space has been proposed in 2017 by Montanino, Vazza, Mirizzi and Viel [64]. Instead of employing some sort of domain-like model for \mathbf{B}_{ext} they rely upon the magnetohydrodynamic cosmological simulations [65, 66]. This issue has been carefully discussed in [28], and so we briefly recall our main conclusions.

Basically, the underlying logic can be summarized as follows. Starting from an arbitrary value B_* of a supposedly existent cosmological magnetic field during the dark age, its evolution as driven by structure formation up to the present is investigated. Denoting by B_0 its present value, a normalization must be fixed in some way, and – once that is done – a prediction for the magnetic field \mathbf{B}_{fil} inside filaments in the present Universe emerges. Concerning the normalization, it is assumed that B_0 should reproduce the magnetic field \mathbf{B}_{clus} of regular clusters today. But a component of \mathbf{B}_{clus} is certainly due to outflows from the cluster galaxies – as demonstrated by the observation of strong iron lines – thereby implying $B_0 < B_{\text{clus}}$. Moreover, it has been shown that strength and structure of \mathbf{B}_{clus} are well reproduced for a wide range of the model parameters by galactic outflows [67, 68]. Thus, one runs the risk to get $B_0 = 0$!

Photon/ALP beam propagation in the Milky Way – We denote by \mathcal{R}_{MW} the region where the photon/ALP beam propagates inside the Milky Way, i.e. from y_{MW} up to the Earth, whose position is denoted by y_{\oplus} .

We compute $\mathcal{U}_{\mathcal{R}_{\text{MW}}}(\mathcal{E}; y_{\oplus}, y_{\text{MW}})$ by closely following the strategy described in [69]. Specifically, in order to take into account the structured behaviour of the Galactic magnetic field \mathbf{B}_{MW} we adopt the recent Jansson and Farrar model [16, 17], which includes a disk and a halo component, both parallel to the Galactic plane, and poloidal ‘X-shaped’ component at the galactic center. Its latest update version is described in [70], where newer polarized synchrotron data and use of different models of the cosmic ray and thermal electron distribution are exploited.

While this model allows also for a random and a striated component of the field, it turns out that only the regular component is relevant in the present context, since the $\gamma \leftrightarrow a$ oscillation length is much larger than the coherence length of the turbulent field.

Inside the Milky Way disk the electron number density is $n_e \simeq 1.1 \times 10^{-2} \text{ cm}^{-3}$, resulting in a plasma frequency $\omega_{\text{pl}} \simeq 4.1 \times 10^{-12} \text{ eV}$: this results from a new model for the distribution of the free electrons in the Galaxy [71]. The Galactic model has an extended thick disk representing the so-called warm interstellar medium, a thin disk representing the Galactic molecular ring, spiral arms based on a recent fit to Galactic HII regions, a Galactic Center disk and seven local features including the Gum Nebula, the Galactic Loop I and the Local Bubble. An offset of the Sun from the Galactic plane and a warp of the outer Galactic disk are included in the model. The parameters of the Galactic model are determined by fitting to 189 pulsars with independently determined distances and DMs.

Thanks to this procedure, we can compute $\mathcal{U}_{\mathcal{R}_{\text{MW}}}(\mathcal{E}; y_{\oplus}, y_{\text{MW}})$ for an arbitrary direction of the line of sight to a given blazar.

Overall photon survival probability – Once all transfer matrices in each region are known, the total transfer matrix \mathcal{U} accounting for the propagation of the photon/ALP beam from the VHE photon production region in the BL Lac jet

up to the Earth reads

$$\mathcal{U}(\mathcal{E}; y_{\oplus}, y_{\text{VHE}}) = \mathcal{U}_{\mathcal{R}_{\text{MW}}}(\mathcal{E}; y_{\oplus}, y_{\text{MW}}) \times \mathcal{U}_{\mathcal{R}_{\text{ext}}}(\mathcal{E}; y_{\text{MW}}, y_{\text{out,host}}) \mathcal{U}_{\mathcal{R}_{\text{host}}}(\mathcal{E}; y_{\text{out,host}}, y_{\text{jet}}) \mathcal{U}_{\mathcal{R}_{\text{jet}}}(\mathcal{E}; y_{\text{jet}}, y_{\text{VHE}}), \quad (9)$$

where of course we have $y_{\text{in,host}} \equiv y_{\text{jet}}$. Since photon polarization cannot be measured in the VHE gamma-ray band, we have to treat the beam as unpolarized. Therefore, we must use the generalized polarization density matrix $\rho(y) = (A_x(y), A_z(y), a(y))^T \otimes (A_x(y), A_z(y), a(y))$. As a consequence, the overall photon survival probability takes the form

$$P_{\gamma \rightarrow \gamma}^{\text{ALP}}(\mathcal{E}; y_{\oplus}, \rho_x, \rho_z; y_{\text{VHE}}, \rho_{\text{unp}}) = \sum_{i=x,z} \text{Tr} [\rho_i \mathcal{U}(\mathcal{E}; y_{\oplus}, y_{\text{VHE}}) \rho_{\text{unp}} \mathcal{U}^\dagger(\mathcal{E}; y_{\oplus}, y_{\text{VHE}})] , \quad (10)$$

where $\rho_x \equiv \text{diag}(1, 0, 0)$, $\rho_z \equiv \text{diag}(0, 1, 0)$ and $\rho_{\text{unp}} \equiv \text{diag}(0.5, 0.5, 0)$. Below – merely for notational convenience – we shall replace $P_{\gamma \rightarrow \gamma}^{\text{ALP}}(\mathcal{E}; y_{\oplus}, \rho_x, \rho_z; y_{\text{VHE}}, \rho_{\text{unp}})$ simply by $P_{\gamma \rightarrow \gamma}^{\text{ALP}}(\mathcal{E}, z)$.

Blazar spectra – We are now in position to use the overall photon survival probability in order to compute the SED νF_ν from the observed spectra of some blazars (Markarian 501, 1ES 0229+200 and a similar source located at $z = 0.6$) in the presence of $\gamma \leftrightarrow a$ oscillations all the way from inside the blazar to us, and we compare our findings with the results from conventional physics.

As a preliminary step, we define the (intrinsic or observed) blazar photon spectrum as

$$\mathcal{F}(\mathcal{E}) \equiv \frac{dN}{dt dA d\mathcal{E}}, \quad (11)$$

where N is the VHE photon number and dA is an infinitesimal area.

For the three considered blazars we model their intrinsic spectrum with a power law exponentially truncated at a fixed cut-off energy \mathcal{E}_{cut} as

$$\mathcal{F}_{\text{int}}(\mathcal{E}) = \mathcal{F}_0 \left(\frac{\mathcal{E}}{\mathcal{E}_0} \right)^{-k} e^{-\mathcal{E}/\mathcal{E}_{\text{cut}}}, \quad (12)$$

where \mathcal{F}_0 is a normalization constant accounting for the blazar luminosity, \mathcal{E}_0 is a reference energy and k is a spectral index. By means of $P_{\gamma \rightarrow \gamma}^{\text{ALP}}$ in Eq. (10) the observed blazar spectrum turns out to be

$$\mathcal{F}_{\text{obs}}(\mathcal{E}) = P_{\gamma \rightarrow \gamma}^{\text{ALP}}(\mathcal{E}) \mathcal{F}_{\text{int}}(\mathcal{E}). \quad (13)$$

In Eq. (10) we use our benchmark values of the free parameters, namely $g_{a\gamma\gamma} = 10^{-11} \text{ GeV}^{-1}$, $B_{T, \mathcal{R}_{\text{VHE}}} = 0.5 \text{ G}$, $B_{\text{ext}} = 1 \text{ nG}$ and $m_a \simeq 10^{-10} \text{ eV}$.

Before proceeding further, we recall that the SED is related to $\mathcal{F}_{\text{obs}}(\mathcal{E})$ by

$$\nu F_\nu = \mathcal{E}^2 \mathcal{F}_{\text{obs}}(\mathcal{E}). \quad (14)$$

The observable physical quantity is the blazar spectrum pertaining to a single random realization of the photon/ALP propagation process. Nevertheless, it is enlightening to evaluate several realizations at once and to compute some of their statistical properties – the median and the area containing the 68%, 90% and 99% of the total number of realizations – in order to check the stability of the result against the distribution of the B_{ext} orientation angles and of L_{dom} , which are indeed random variables.

- *Markarian 501* – Markarian 501 is a high-frequency peaked blazar (HBL) observed in the sky at RA : 16 h 53 m 52.2 s and DEC : +39 d 45 m 37 s at a redshift $z = 0.034$. We use the observational data points from HEGRA [72] in a condition where Markarian 501 was observed in a high emission state, thereby allowing us to have a very good description of its spectrum up to $\sim 30 \text{ TeV}$. This fact is important for testing our model, since at such high energies it starts to give different predictions with respect to conventional physics. In Figure 1 we report its observed SED both when only conventional physics is considered and when $\gamma \leftrightarrow a$ oscillations are at work. In order to obtain the SED we take $\mathcal{E}_{\text{cut}} = 10 \text{ TeV}$, $\mathcal{E}_0 = 1 \text{ TeV}$ and $k = 1.8$ in Eq. (12).

- *1ES 0229+200* – 1ES 0229+200 is a BL Lac observed in the sky at RA : 02 h 32 m 48.6 s and DEC : +20 d 17 m 17 s at a redshift $z = 0.1396$. 1ES 0229+200 is the prototype of the so-called ‘extreme HBL’ (EHBL) [73, 74] which shows a rather hard VHE observed spectrum up to at least 10 TeV. This fact is particularly interesting since the observed data points at such high energies can start to distinguish between different models (conventional physics versus photon-ALP oscillations). Future observations with the CTA that can eventually reach energies up to 100 TeV could give a definitive answer. In Figure 2 we plot its observed SED both when only conventional physics is taken into account and in the case in which also $\gamma \leftrightarrow a$ oscillations are present. The SED is obtained by taking in Eq. (12) $\mathcal{E}_{\text{cut}} = 30$ TeV in the case of conventional physics and $\mathcal{E}_{\text{cut}} = 10$ TeV when $\gamma \leftrightarrow a$ oscillations are taken into account, $\mathcal{E}_0 = 1$ TeV and $k = 1.4$.
- *Extreme BL Lac at $z = 0.6$* – BL Lacs have been observed also at redshift $z \geq 0.6$: we assume the existence of an EHBL at a redshift $z = 0.6$. For this blazar we suppose a SED similar to the one of 1ES 0229+200 which is the prototype of EHBLs so that we take $\mathcal{E}_{\text{cut}} = 30$ TeV, $\mathcal{E}_0 = 1$ TeV and $k = 1.4$ in Eq. (12). We consider two cases: 1) we imagine that such BL Lac is observed in the sky along the direction of the galactic pole: in Figure 3 we plot its observed SED both when only conventional physics is taken into account and in the case in which also $\gamma \leftrightarrow a$ oscillations are present; 2) we hypothesize that the same BL Lac is instead observed in the sky along the direction of the galactic plane: in Figure 4 we exhibit the corresponding observed SED according to conventional physics and when $\gamma \leftrightarrow a$ oscillations are considered.

Figures are reported after the bibliography.

Results – Figures 1-4 show our results about the SED of the above-considered BL Lacs. As a general outcome, we get that the $\gamma \leftrightarrow a$ oscillations allow for a harder observed spectra for all sources as compared with the results of conventional physics. In particular, this fact becomes more and more evident as \mathcal{E} or z (or both) increase.

We infer from our findings that $\gamma \rightarrow a$ conversions inside the magnetic field of the BL Lac jet can be very important in order to start the propagation in the extragalactic space with a certain amount of already produced ALPs: its relevance depends both on \mathcal{E} and on z . This point is rather subtle and deserves a clear explanation. Superficially, one might expect $P_{\gamma \rightarrow \gamma}^{\text{ALP}}(\mathcal{E}, z)$ to increase with $g_{a\gamma\gamma}$, in line with physical intuition. This is certainly true as long as the EBL plays an insignificant role, namely for \mathcal{E} and z low enough. Needless to say, $\gamma \rightarrow a$ conversions and $a \rightarrow \gamma$ back-conversion in the BL Lac and in the Milky Way can help increasing $P_{\gamma \rightarrow \gamma}^{\text{ALP}}(\mathcal{E}, z)$, but not that much. Consider next the situation in which both $g_{a\gamma\gamma}$ and z are fairly large – say $z = 0.6$ – but \mathcal{E} is not, so that photon dispersion on the CMB can be neglected. In such a situation the conversion probability gets enhanced: inside a single magnetic domain many $\gamma \rightarrow a$ and $a \rightarrow \gamma$ conversions take place. But since z is supposed to be rather large the EBL level is high, which causes most of the photons to be absorbed. Such a behaviour is very clearly exhibited in Figures 3 and 4 around $\mathcal{E} \simeq 3$ TeV. As the energy increases photon dispersion on the CMB becomes dominant: now a much smaller number of $\gamma \rightarrow a$ and $a \rightarrow \gamma$ conversions occurs. As a consequence, most of the ALPs produced in the BL Lac survive until they enter the Galaxy, whose strong magnetic field allows them to convert to photons. This fact explains the peak in Figures 3 and 4 around $\mathcal{E} = (10 - 30)$ TeV. From all the figures we observe that as \mathcal{E} progressively increases beyond 70 TeV the area covered by the various realizations of the photon/ALP propagation process gradually reduces. The reason for this fact is that the EBL absorption is so high at those energies that almost all the photons in each extragalactic magnetic field domain are absorbed and only the ones reconverted from ALPs in the domains closest to the Earth survive, as previously mentioned. As a result, the parameter space of the model (B_{ext} orientation angles, domain lengths L_{dom}) gets reduced, and this fact decreases the available area that can be covered by the single realizations of the propagation.

Conclusions – In this Letter, we have studied the propagation of a photon/ALP beam originating well inside a BL Lac jet and traveling in the jet magnetic field, in the host galaxy magnetic field, in the extragalactic magnetic field, and in the Milky Way magnetic field up to us. We observe from Markarian 501 (see Figure 1) that conventional physics hardly fits the two highest energy points of the SED while the model including $\gamma \leftrightarrow a$ oscillations naturally matches the data. The same is true for 1ES 0229+200 concerning the last highest energy data point of the SED. As it is evident from Figures 3 and 4 – as the redshift increases – at high energies the difference between results from conventional physics alone and the model including $\gamma \leftrightarrow a$ oscillations becomes more and more dramatic. This is even more the case when sizable $\gamma \rightarrow a$ conversions take place inside a blazar, since then most of the emitted ALPs can become photons only inside the strong Milky Way magnetic field. In addition, the energy oscillations in the observed spectrum – clearly recognizable in the Figures – are a clear-cut feature of our scenario, which can be observed provided that the detector has enough energy resolution: they arise from the photon dispersion on the CMB. Thus, our predictions are of great importance for the new generation of gamma-ray observatories like CTA

(Cherenkov Telescope Array) [4], HAWC (High-Altitude Water Cherenkov Observatory) [75], GAMMA 400 (Gamma-Astronomy Multifunction Modules Apparatus) [76], LHAASO (Large High Altitude Air Shower Observatory) [77], TAIGA-HiSCORE (Tunka Advanced Instrument for Gamma-ray and Cosmic ray Astrophysics-Hundred Square km Cosmic ORigin Explorer) [78] and HERD (High Energy cosmic-Radiation Detection) [79], which can test our model and eventually make a first indirect detection of an ALP with properties similar to the ones described in this Letter. We plan to perform dedicated simulations in order to test in BL Lac spectra the detectability with CTA of energy oscillations around 500 GeV – 2 TeV and/or photon excess at about 10 – 30 TeV.

Still, this is not the end of the story. Because our ALP has mass $m_a \lesssim 10^{-10}$ eV and assuming that indeed $g_{a\gamma\gamma} \simeq 10^{-11} \text{ GeV}^{-1}$, it can be directly detected in the laboratory within the next few years, thanks to the upgrade of ALPS II at DESY [80], the planned IAXO [81] and STAX [82] experiments, as well as with other techniques developed by Avignone and collaborators [83–85]. Moreover, if the bulk of the dark matter is made of ALPs they can also be detected by the planned ABRACADABRA experiment [86].

Finally, we plan to consider a much larger number of blazars – both observed and simulated – in a more complete and systematic forthcoming publication.

Acknowledgments – G. G. and F. T. acknowledge contribution from the grant INAF CTA-SKA, ‘Probing particle acceleration and γ -ray propagation with CTA and its precursors’, M. R. acknowledges the financial support by the TAsP grant of INFN and C. E. acknowledges the European Commission for support under the H2020-MSCA-IF-2016 action, Grant No. 751311 ‘GRAPES Galactic cosmic RAY Propagation: An Extensive Study’.

-
- [1] <https://www.mpi-hd.mpg.de/hfm/HESS>
 - [2] <https://magic.mpp.mpg.de/>
 - [3] <http://veritas.sao.arizona.edu/>
 - [4] <https://www.cta-observatory.org/>
 - [5] E. Dwek and F. Krennrich, *Astropart. Phys.* **43**, 112 (2013).
 - [6] G. Breit and J. A. Wheeler, *Phys. Rev.* **46**, 1087 (1934).
 - [7] W. Heitler, *The Quantum Theory Of Radiation* (Oxford University Press, Oxford, 1960).
 - [8] R. J. Gould and G. P. Schre’der, *Phys. Rev.* **155**, 1408 (1967)
 - [9] G. G. Fazio and F. W. Stecker, *Nature* **226**, 135 (1970).
 - [10] A. De Angelis, G. Galanti and M. Roncadelli, *Mon. Not. R. Astron. Soc.* **432**, 3245 (2013).
 - [11] A. De Angelis, M. Roncadelli and O. Mansutti, *Phys. Rev. D* **76**, 121301 (2007).
 - [12] M. Simet, D. Hooper and P. D. Serpico, *Phys. Rev. D* **77**, 063001 (2008).
 - [13] M. A. Sánchez-Conde *et al.*, *Phys. Rev. D* **79**, 123511 (2009).
 - [14] A. Dobrynina, A. Kartavtsev, and G. Raffelt, *Phys. Rev.* **91** (2015) 083003; **91**, 109902 (E) (2015).
 - [15] A. Franceschini and G. Rodighiero, *Astron. Astrophys.* **603**, 34 (2017).
 - [16] R. Jansson and G. R. Farrar, *Astrophys. J.* **757**, 14 (2012).
 - [17] R. Jansson and G. R. Farrar, *Astrophys. J.* **761** L11 (2012).
 - [18] J. Jaeckel and A. Ringwald, *Ann. Rev. Nucl. Part. Sci.* **60**, 405 (2010).
 - [19] A. Ringwald, *Phys. Dark Univ.* **1**, 116 (2012).
 - [20] J.E. Kim, G. Carosi, *Rev. Mod. Phys.* **82**, 557601 (2010).
 - [21] P. Sikivie, *Phys. Rev. Lett.* **51**, 1415 (1983); (E) *ibid.* **52**, 695 (1984).
 - [22] A. A. Anselm, *Yad. Fiz.* **42**, 1480 (1985).
 - [23] G. G. Raffelt, L. Stodolsky, *Phys. Rev. D* **37**, 1237 (1988).
 - [24] W. Heisenberg, H. Euler, *Z. Phys.* **98**, 714732 (1936).
 - [25] V.S. Weisskopf, K. Dan, *Vidensk. Selsk. Mat. Fys. Medd.* **14**, 6 (1936).
 - [26] J. Schwinger, *Phys. Rev.* **82**, 664679 (1951).
 - [27] A. De Angelis, G. Galanti, M. Roncadelli, *Phys. Rev. D* **84**, 105030 (2011); (E) *ibid.* **84** 105030 (2013).
 - [28] G. Galanti and M. Roncadelli, *Phys. Rev. D* **98**, 043018 (2018).
 - [29] V. Anastassopoulos *et al.* [CAST Collaboration], *Nature Physics* **13**, 584 (2017).
 - [30] A. Ayala *et al.*, *Phys. Rev. Lett.* **113**, 191302 (2014).
 - [31] D. Wouters, P. Brun, *Phys. Rev. D* **86**, 043005 (2012).
 - [32] A. Abramowski *et al.* [HESS Collaboration], *Phys. Rev. D* **88**, 102003 (2013).
 - [33] G. Galanti, M. Roncadelli, arXiv:1305.2114.
 - [34] M. C. D. Marsh *et al.*, *JCAP* **12**, 036 (2017).
 - [35] M. Ajello *et al.*, [Fermi-LAT collaboration], *Phys. Rev. Lett.* **116**, 161101 (2016).
 - [36] C. Zhang *et al.*, arXiv:1802.0420.
 - [37] T. Moroi, K. Nakayama and Y. Tang, arXiv:1804.10378.
 - [38] D. Malyshev *et al.*, arXiv:1805.04388.
 - [39] J. W. Brockway, E. D. Carlson, and G. G. Raffelt, *Phys. Lett. B* **383**, 439 (1996).

- [40] J. A. Grifols, E. Massó and R. Toldrà, *Phys. Rev. Lett.* **77**, 2372 (1996).
- [41] A. Payez *et al.*, *JCAP* **02**, 006 (2015).
- [42] G. G. Raffelt, *Stars as Laboratories for Fundamental Physics* (The University of Chicago Press, Chicago, 1996).
- [43] S. Stetina, E. Rrapaj and S. Reddy, *Phys. Rev D* **78**, 064056 (2008).
- [44] F. Tavecchio, M. Roncadelli and G. Galanti, *Phys. Lett. B* **744**, 375 (2015).
- [45] F. Tavecchio *et al.*, *Mon. Not. R. Astron. Soc.* **401**, 1570 (2010).
- [46] M. C. Begelman, R. D. Blandford, M. J. Rees, *Rev. Mod. Phys.* **56**, 255 (1984).
- [47] G. Ghisellini, F. Tavecchio, *Mon. Not. R. Astron. Soc.* **397**, 985 (2009).
- [48] R. E. Pudritz, M. J. Hardcastle, D. C. Gabuzda, *Space Sci. Rev.* **169**, 27 (2012).
- [49] D. Moss and A. Shukurov, *Mon. Not. R. Astron. Soc.* **279**, 229 (1996).
- [50] F. Tavecchio, M. Roncadelli, G. Galanti and G. Bonnoli, *Phys. Rev. D* **86**, 085036 (2012).
- [51] A. Kartavtsev, G. Raffelt and H. Vogel, *JCAP* **01**, 024 (2017).
- [52] G. Galanti and M. Roncadelli, *JHEA* **20**, 1 (2018).
- [53] P. P. Kronberg, *Rept. Prog. Phys.* **57**, 325 (1994).
- [54] D. Grasso and H. R. Rubinstein, *Phys. Rep.* **348**, 163 (2001).
- [55] C. Wang and D. Lai, *JCAP* **16**, 006 (2016).
- [56] E. Masaki, A. Aoki and J. Soda, arXiv:1702.08843.
- [57] A. Neronov and I. Vovk, *Science* **328**, 73 (2010).
- [58] R. Durrer and A. Neronov, *Astron. Astrophys. Rev.* **21**, 62 (2013).
- [59] M. S. Pshirkov, P. G. Tinyakov and F. R. Urban, *Phys. Rev. Lett.* **116**, 191302 (2016).
- [60] M. J. Rees and G. Setti, *Nature* **219**, 127 (1968).
- [61] F. Hoyle, *Nature* **223**, 936 (1969).
- [62] S. Furlanetto and A. Loeb, *Astrophys. J.* **556**, 619 (2001).
- [63] P. P. Kronberg, H. Lesch and U. Hopp, *Astrophys. J.* **511**, 56 (1999).
- [64] D. Montanino, F. Vazza, A. Mirizzi and M. Viel, *Phys. Rev. Lett.* **119**, 101101 (2017).
- [65] F. Vazza, M. Brüggen, C. Gheller and P. Wang, *Mon. Not. Roy. Astron. Soc.* **445**, 3706 (2014).
- [66] C. Gheller *et al.*, *Mon. Not. R. Astron. Soc.* **462**, 448 (2016).
- [67] Xu H., Li H., Collins D. C., Li S., Norman M. L., *Astrophys. J. Lett.* **698**, L14 (2009).
- [68] J. Donnert, K. Dolag, H. Lesch and E. Müller, *Mon. Not. R. Astron. Soc.* **392**, 1008 (2009).
- [69] D. Horns, L. Maccione, M. Meyer, A. Mirizzi, D. Montanino, and M. Roncadelli, *Phys. Rev. D* **86**, 075024 (2012).
- [70] M. Unger and G. R. Farrar, arXiv:1707.02339.
- [71] J. M. Yao, R. N. Manchester and N. Wang, *Astrophys. J.* **835**, 29 (2017).
- [72] F. Aharonian *et al.*, *Astrophys. J.* **546**, 898 (2001).
- [73] G. Bonnoli, F. Tavecchio, G. Ghisellini and T. Sbarrato, *Mon. Not. R. Astron. Soc.* **451**, 611 (2015).
- [74] L. Costamante, G. Bonnoli, F. Tavecchio, G. Ghisellini, G. Tagliaferri and D. Khangulyan, *Mon. Not. R. Astron. Soc.* **477**, 4257 (2018).
- [75] www.hawc-observatory.org/.
- [76] gamma400.lebedev.ru/gamma400e.html.
- [77] <http://english.ihep.cas.cn/ic/ip/LHAASO/>.
- [78] www.desy.de/groups/astroparticle/score/en/.
- [79] X. Huang *et al.*, *Astropart. Phys.* **78**, 35 (2016).
- [80] R. Bähre *et al.*, *J. of Instrum.* **8**, T09001 (2013).
- [81] I. G. Irastorza *et al.* [IAXO Collaboration], *JCAP* **06**, 013 (2011).
- [82] L. M. Capparelli *et al.*, *Phys. Dark Univ.* **12**, 37 (2016).
- [83] F. T. Avignone III, *Phys. Rev. D* **79**, 035015 (2009).
- [84] F. T. Avignone III, R. J. Crewick and S. Nussinov, *Phys. Lett. B* **681**, 122 (2009).
- [85] F. T. Avignone III, R. J. Crewick and S. Nussinov, *Astropart. Phys.* **34**, 640 (2011).
- [86] Y. Kahn, B. R. Safdi and J. Thaler, *Phys. Rev. Lett.* **117**, 141801 (2016).
- [87] Ie. Vovk, A. M. Taylor, D. Semikoz and A. Neronov, *Astrophys. J.* **747**, L14 (2012).
- [88] F. Aharonian *et al.* [H.E.S.S. Collaboration], *Astron. Astrophys.* **475**, L9 (2007).

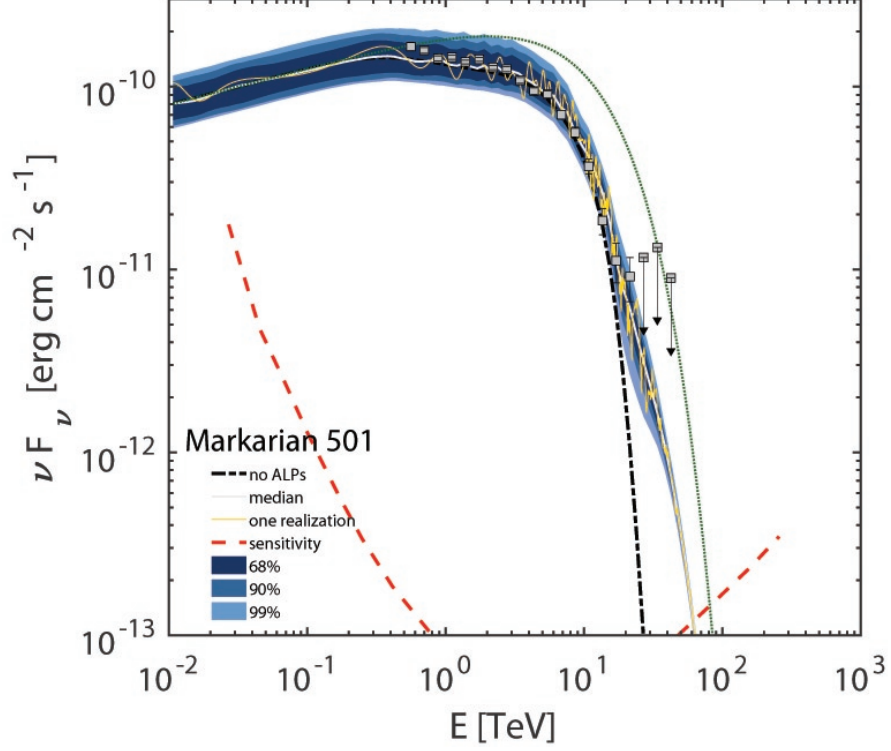


FIG. 1: Behaviour of the observed SED of Markarian 501 versus the observed energy \mathcal{E} . The dotted-dashed black line corresponds to conventional physics, the solid light-gray line to the median of all the realizations of the photon/ALP propagation process and the solid yellow line to a single realization with a random distribution of the domain lengths and of the orientation angles of the extragalactic magnetic field. The dotted green line is the intrinsic SED and the dashed red line represents the CTA sensitivity. The filled area is the envelope of the results on the percentile of all the possible realizations of the propagation process at 68% (dark blue), 90% (blue) and 99% (light blue), respectively. The light gray filled squares are the spectrum detected by HEGRA [72].

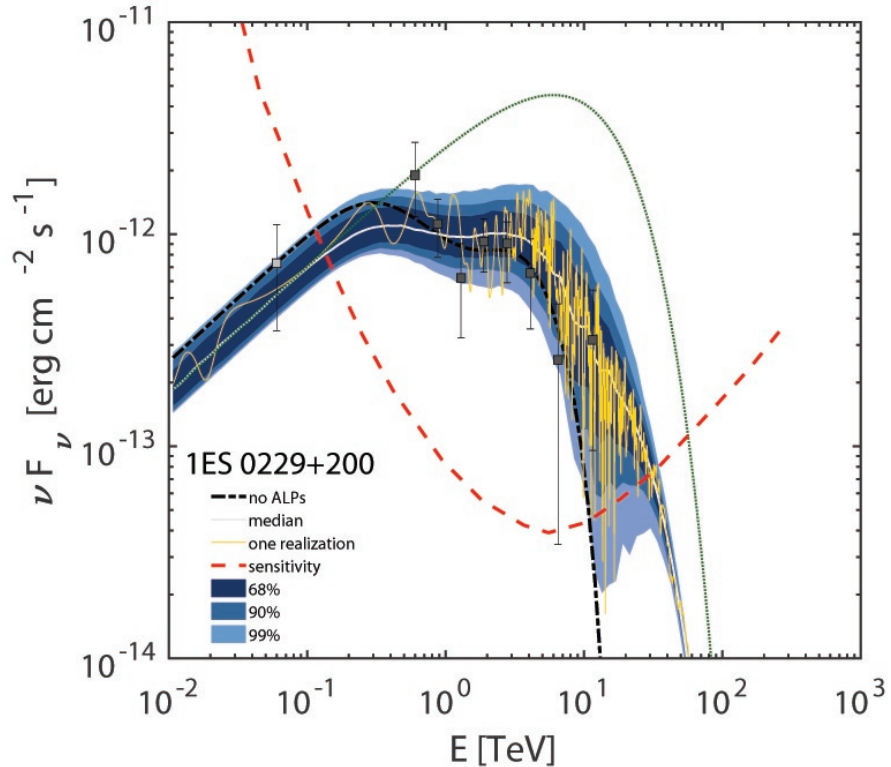


FIG. 2: Same as Figure 1 but for 1ES 0229+200. The light gray filled squares are the spectrum detected by Fermi/LAT [87].

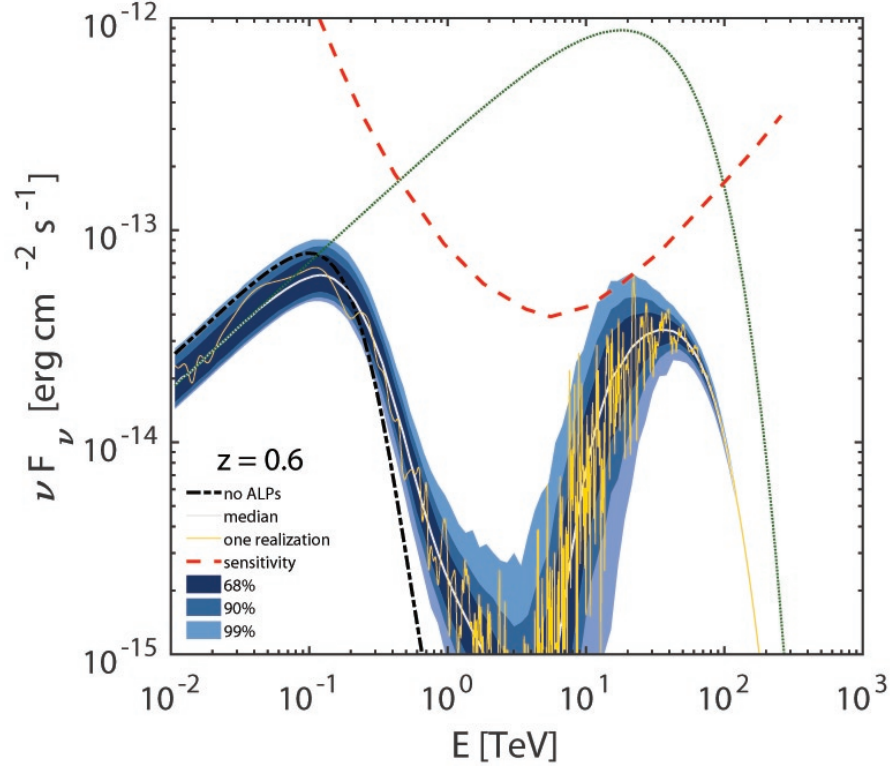


FIG. 3: Same as Figure 1 but for a BL Lac at $z = 0.6$ in the case of observation of the BL Lac along the direction of the galactic pole.

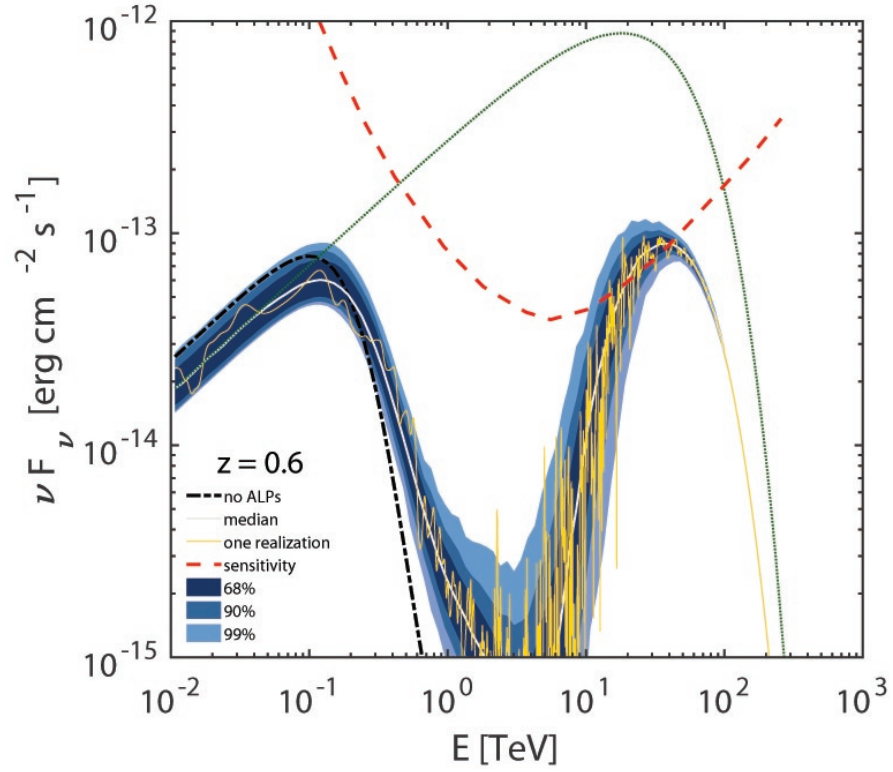


FIG. 4: Same as Figure 1 but for a BL Lac at $z = 0.6$ in the case of observation of the BL Lac along the direction of the galactic plane.